Mapping the high ionization rate of the GC starburst Sgr B2 through low HCO^+ / N_2H^+ J=1-0 intensity ratios

Miriam G. Santa-Maria[1,*] and *Javier* R. Goicoechea[1]

[1]Instituto de Física Fundamental (IFF), CSIC. Calle Serrano 121-123, 28006 Madrid, Spain

Abstract. We still do not understand which mechanisms dominate the heating and ionization of the extended molecular gas in galactic nuclei. The starburst Sgr B2, in the Galactic Center (GC), is an excellent template to spatially resolve the high-mass star-forming cores from the extended cloud environment, and to study the properties of the warm neutral gas in conditions likely prevalent in star-forming galaxies. We mapped ∼1000 pc^2 of Sgr B2 complex, using the IRAM 30m telescope, in the N_2H^+, HCO^+ J=1-0 and SiO J=2-1 line emission. The extended nature of the N_2H^+ J=1-0 emission is remarkable. Compared to molecular clouds in the disk of the galaxy, the N_2H^+ J=1-0 emission is not confined to cold and dense cores and filaments. This can be explained by the high ionization rate ($\zeta \gtrsim 10^{-15}$ s^{-1}), leading to overabundant H_3^+, He^+, and N_2H^+. The enhanced ionization rate is likely responsible of the much lower line intensity ratio $R_I = HCO^+/N_2H^+$ J=1-0 observed in Sgr B2 ($R_I \approx 2 \pm 2$), Arp 220 ($R_I \approx 2$), and NGC 253 ($R_I \approx 5$), compared to disk clouds such as Orion B ($R_I \approx 24$) and starburst galaxies such as M82 ($R_I \approx 21$).

1 Introduction

The conditions prevailing in the interstellar medium (ISM) of galactic nuclei can be extreme compared to those in the more quiescent disk of galaxies. Such conditions are regulated by the feedback from OB-type stars: strong UV radiation fields, stellar winds, and supernovae explosions [1]; cloud-cloud collisions [2], enhanced cosmic ray (CR) fluxes [3], and X-ray emission (from accretion onto a super-massive black hole, SMBH) [4]. To understand star formation in these environments, and galaxy evolution in general, it is critical to characterize the gas heating and ionization mechanisms in the ISM of galactic nuclei.

Sagittarius B2 is the most massive and far-infrared (FIR) luminous (∼10^7 $L_\odot$) molecular cloud in the Galactic Center (GC). It shows ongoing high-mass star formation and line-of-sight column densities above $N_{H_2} \gtrsim 10^{24}$ cm^{-2} [3]. Sgr B2 is located at a projected distance of about 100 pc from the dynamical center of the Milky Way (Sgr A*) [5]. It contains three main high-mass star-forming cores (named N, M, and S), with more than 49 compact H II regions [6] embedded in a moderately high density ($n(H_2) \gtrsim 10^5$ cm^{-3}) molecular cloud which is surrounded by a more extended and lower density envelope, hereafter "Sgr B2 envelope" [7].

It is a long-standing debate whether radiation, CRs, or shocks dominate the heating of the widespread warm molecular gas in the Sgr B2 complex. Plausible candidates are: cloud-cloud collisions [2, 8], UV-irradiated low-velocity shocks [9], X-rays from brief outburst periods of Sgr A*, or low-energy cosmic ray (LECRs) showers [4].

*e-mail: miriam.g.sm@csic.es

Variations in the abundances of particular molecular ions, such as the HCO^+ over N_2H^+ abundance ratio, help to constrain the ionization processes that result from X-ray and LECRs irradiation [10]. In this paper we briefly summarize the main results of our IRAM 30m mapping study of Sgr B2 complex, focusing on the characteristics of the N_2H^+ and HCO^+ J=1-0 emission.

2 Mapping observations

We mapped Sgr B2 in the 3mm band (~90 GHz) using the IRAM 30m telescope. The size of our maps is $12' \times 12'$ (see Fig. 1). The angular resolution at the target frequencies is $\sim 27''$ (~ 1 pc at the distance to Sgr B2). We complement these observations with *NuSTAR* hard X-rays (3-78 keV) continuum observations. However, these X-rays observations are not conclusive of whether Sgr B2 is (still) reprocessing X-rays from past flaring activity of Sgr A* or if (the observed) X-rays arise from LECRs [4, 12]. In this work we refer to the ionization rate (ζ), without distinction between X-rays and CRs ionization rate.

3 Widespread N_2H^+ emission far from star-forming cores

The observed N_2H^+ J=1-0 emission is extended at pc scales. This is an unexpected result as in nearby molecular clouds of the Galactic disk the N_2H^+ emission is confined to dense filaments and cold prestellar cores inside them [13]. The common interpretation is that N_2H^+ traces very dense gas at high extinction depths, that is, cold gas ($T_k < 20$ K) shielded from

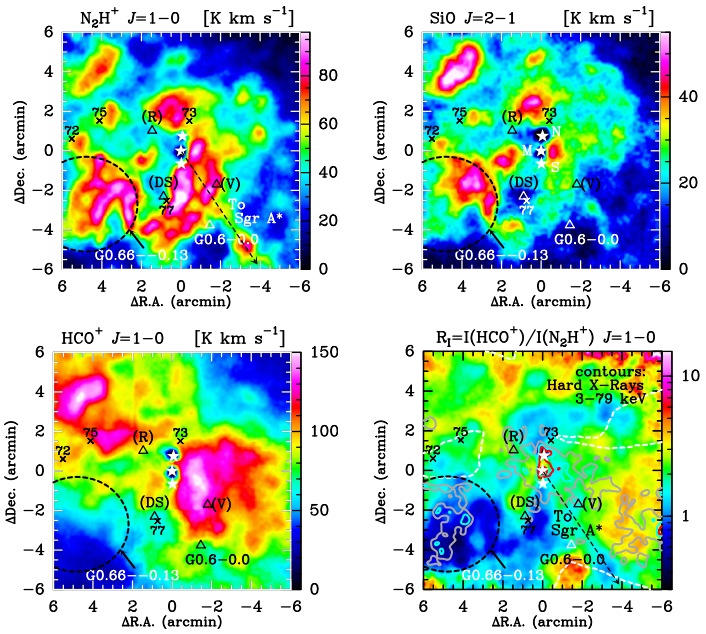

Figure 1. IRAM 30m total line intensity maps (in K km s^{-1}): N_2H^+, HCO^+ J=1-0 and SiO J=2-1 integrated in the LSR velocity range [-20, 120] km s^{-1}. *Bottom-right*: R_1=I(HCO^+)/I(N_2H^+) J=1-0 intensity ratio. The three white stars mark the position of the main star-forming cores (N, M, S). Triangles mark other H II regions. Black dashed circle marks an X-ray irradiated region [4]. Contours on the R_1 map show the hard X-ray emission published in 2015 [4]. Dashed white lines delineate the regions with no X-ray observations. The X symbols and the numbers are *NuSTAR* X-ray point sources [11].

stellar FUV radiation where CO freezes-out on dust grains [14]. In Sgr B2, however, the N_2H^+ emission is remarkably widespread and extended. In addition, it spatially correlates with the SiO J=2-1 emission (see Fig. 1; $\rho_{sp} = 0.7$ [3]), considered to be tracer of warm shocked gas.

The main formation route of N_2H^+ is reaction of H_3^+ with N_2 (the major gas-phase nitrogen reservoir inside molecular clouds). Its main destruction route is reacting with CO,

$$N_2 + H_3^+ \rightarrow N_2H^+ + H_2, \quad (1)$$
$$N_2H^+ + CO \rightarrow HCO^+ + N_2. \quad (2)$$

H_3^+ forms after H_2 ionization and drives the production of molecular ions in dense interstellar clouds [15]. The ionization rate in Sgr B2 is high, $\zeta \simeq (1\text{-}10)\times10^{-15}$ s^{-1} [4], about 10-100 times higher than that in typical molecular clouds of the Galactic disk. This enhanced rate increases the H_3^+ and He^+ production rate, but also the destruction rate of CO through gas-phase reactions with H_3^+ and He^+:

$$H_3^+ + CO \rightarrow HCO^+ + H_2, \quad (3)$$
$$He^+ + CO \rightarrow C^+ + O + He \ \text{ or } \ C + O^+ + He. \quad (4)$$

In addition, He^+ reacts with N_2 to form N_2^+, which then reacts with H_2 to form more N_2H^+. For high values of ζ, the ionization fraction, $x_e = n_e/n_H$, is also high. This implies that N_2H^+ and HCO^+ start to be destroyed by dissociative recombinations with electrons. In consequence, the column density ratio R_N=$N(HCO^+)/N(N_2H^+)$ decreases as ζ increases (see also [10]). This reasoning applies as long as the destruction of H_3^+ is dominated by reactions with CO (so-called "low ionization phase", LIP) and not by recombinations with electrons [16, 17]. In this phase, protonation reactions with H_3^+ dominate the formation of abundant molecular ions such as N_2H^+. Our photochemical models of the Sgr B2 envelope (with $G_0 = 10^3$ and $\zeta \gtrsim 10^{-15}$ s^{-1}; Fig. 2 *left*) show that the N_2H^+ emission must arise from moderately dense gas ($n_H \gtrsim 10^5$ cm^{-3}) and from moderate cloud depths (A_V) so that the CO abundance is higher than x_e.

At low densities ($n_H < 10^4$ cm^{-3}) and high ionization rates ($\zeta \gtrsim 10^{-15}$ s^{-1}) the gas chemistry switches to a phase in which destruction of H_3^+ via electron recombinations is comparable to destruction via reactions with CO. This phase is called "high ionization phase" (HIP). The abundances of molecular ions such as HCO^+ and N_2H^+ are much lower in this phase. It is unlikely that the observed extended N_2H^+ emission in Sgr B2 is in the HIP.

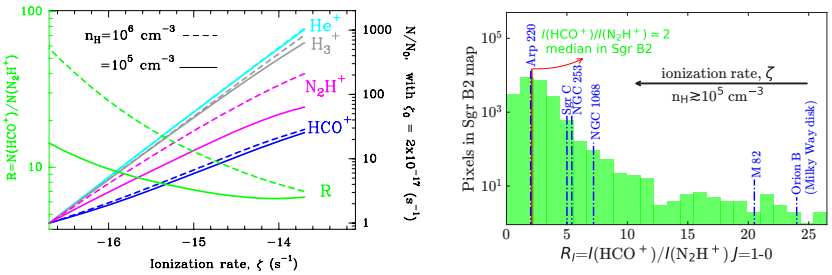

Figure 2. *Left:* Model predictions for different ionization rates, ζ, (constant G_0=10^3, n_H=10^5 and 10^6 cm^{-3}, and $A_{V,tot}$=15 mag). Green curves show the column density ratio R_N. Colored curves (blue, pink, gray, and cyan) show the column density enhancement, N/N_0, with respect to models with ζ_0=2×10^{-17} s^{-1} (average ionization rate in Galactic disk molecular clouds) [3]. *Right:* Histogram of all observed $R_I = I(HCO^+)/I(N_2H^+)$ J=1-0 line intensity ratios in our map of Sgr B2 (green). The black arrow indicates the direction of increasing ionization rate. The red line marks the median value of the intensity ratio in Sgr B2 complex. Dashed blue lines mark the line intensity ratios R_I observed in Orion B at large spatial scales [13], in M 82, NGC 1068, NGC 253, Arp 220 [18], and in Sgr C [19]. Recall that, in general, the value R_N (*left*) is different than R_I (*right*).

3.1 HCO^+/N_2H^+ intensity ratio in Sgr B2 envelope and in other environments

At sufficiently high densities, $n_{\rm H} \gtrsim 10^5$ cm^{-3} and in the LIP phase, the column density ratio R_N (HCO^+/N_2H^+) inversely scales with the ionization rate ζ, and it scales with gas density. In Sgr B2, the R_I(HCO^+/N_2H^+) map (Fig. 1, *bottom-right*) shows low ratios (<1) in specific X-rays irradiated regions (e.g.,G0.66–0.13) but higher ratios in others (e.g.,western regions). The average value of the line intensity ratio R_I is low, $R_I = 2 \pm 2$. This is much lower than that the ratio observed in Orion B averaged over large spatial scales, $R_I \sim 24$ [13]. However, the observed intensity ratio matches that of Arp 220 (a merger ULIRG galaxy). This match suggests similar environmental conditions (Arp 220 possibly hosts thousands of embedded Sgr B2-like starburst regions). NGC 253 (a spiral galaxy with widespread shocks) shows a ratio of $R_I \sim 5$, whereas the starburst galaxy M 82 shows a much higher ratio, $R_I \sim 21$, closer to the values observed in molecular clouds of the galactic disk (i.e., affected by lower ionization rates).

In this study we find that low R_I(HCO^+/N_2H^+) line intensity ratios trace relatively dense molecular gas and high ionization rates (produced by enhanced doses of cosmic rays and X-rays). In Sgr B2, the intensity ratio R_I is low (<1) over large spatial scales. This result suggests that part of the rich and characteristic chemistry of Sgr B2 is produced by the high ionization rate in the GC. This also implies that the emissivity and behavior of certain molecules differ from that in typical molecular clouds of the disk (or in normal galaxies).

In order to determine the column densities of HCO^+ and N_2H^+, and to constrain R_N accurately, one would need to map their higher frequency rotationally excited lines and study their excitation and radiative transfer. Much higher angular resolution maps will allow us to spatially separate the different environments in these complex regions and to dissect their dominant heating and ionization mechanisms.

References

[1] Goicoechea, J. R., Santa-Maria, M. G., Teyssier, D., et al. 2018, A&A, 616, L1
[2] Tsuboi, M., Miyazaki, A., & Uehara, K. 2015, PASJ, 67, 90
[3] Santa-Maria, M. G., Goicoechea, J. R., Etxaluze, M., et al. 2021, A&A, 649, A32
[4] Zhang, S., Hailey, C. J., Mori, K., et al. 2015, ApJ, 815, 132
[5] Molinari, S., Bally, J., Noriega-Crespo, A., et al. 2011, ApJ, 735, L33
[6] Ginsburg, A., Bally, J., Barnes, A., et al. 2018, ApJ, 853, 171
[7] Huttemeister, S., Wilson, T. L., Henkel, C., et al. 1993, A&A, 276, 445
[8] Hasegawa, T., Sato, F., Whiteoak, J. B., et al. 1994, ApJ, 429, L77
[9] Goicoechea, J. R., Rodríguez-Fernández, N. J., & Cernicharo, J. 2004, ApJ, 600, 214
[10] Ceccarelli, C., Dominik, C., López-Sepulcre, A., et al. 2014, ApJL, 790, L1
[11] Hong, J., Mori, K., Hailey, C. J., et al. 2016, ApJ, 825, 132
[12] Kuznetsova, E., Krivonos, R., Lutovinov, A., et al. 2022, MNRAS, 509, 1605
[13] Pety, J., Guzmán, V. V., Orkisz, J. H., et al. 2017, A&A, 599, A98
[14] Caselli, P., Benson, P. J., Myers, P. C., et al. 2002, ApJ, 572, 238
[15] Wolfire, M. G., Vallini, L., & Chevance, M. 2022
[16] Pineau des Forets, G., Roueff, E., & Flower, D. R. 1992, MNRAS, 258, 45P
[17] Le Bourlot, J., Pineau des Forets, G., Roueff, E., et al. 1993, ApJ, 416, L87
[18] Aladro, R., Martín, S., Riquelme, D., et al. 2015, A&A, 579, A101
[19] Jones, P. A., Burton, M. G., Cunningham, M. R., et al. 2012, MNRAS, 419, 2961